Chimeric Anti-CD14 IGG2/4 Hybrid Antibodies for Therapeutic Intervention in Pig and Human Models of Inflammation

Corinna Lau,* Kristin S. Gunnarsen,[†,‡,§] Lene S. Høydahl,[†,‡,§] Jan Terje Andersen,[†,‡,§] Gøril Berntzen,[†,‡,§] Anne Pharo,[‡] Julie K. Lindstad,[‡] Judith K. Ludviksen,* Ole-Lars Brekke,[*,¶] Andreas Barratt-Due,[‡] Erik Waage Nielsen,[*,¶] Christopher R. Stokes,[‖] Terje Espevik,[#] Inger Sandlie,[†,‡,§] and Tom Eirik Mollnes[*,‡,¶,#]

CD14 is a key recognition molecule of innate immune responses, interacting with several TLRs. TLR signaling cross-talks extensively with the complement system, and combined CD14 and complement inhibition has been proved effective in attenuating inflammatory responses. Pig models of human diseases have emerged as valuable tools to study therapeutic intervention, but suitable neutralizing Abs are rare. Undesired Fc-mediated functions, such as platelet activation and IL-8 release induced by the porcine CD14-specific clone Mil2, limit further studies. Therefore, an inert human IgG2/IgG4 hybrid C region was chosen for an rMil2. As revealed in ex vivo and in vivo pig experiments, rMil2 inhibited the CD14-mediated proinflammatory cytokine response similar to the original clone, but lacked the undesired Fc-effects, and inflammation was attenuated further by simultaneous complement inhibition. Moreover, rMil2 bound porcine FcRn, a regulator of $t_{1/2}$ and biodistribution. Thus, rMil2, particularly combined with complement inhibitors, should be well suited for in vivo studies using porcine models of diseases, such as sepsis and ischemia-reperfusion injury. Similarly, the recombinant anti-human CD14 IgG2/4 Ab, r18D11, was generated with greatly reduced Fc-mediated effects and preserved inhibitory function ex vivo. Such Abs might be drug candidates for the treatment of innate immunity-mediated human diseases. ***The Journal of Immunology*****, 2013, 191: 4769–4777.**

CD14 is a pattern recognition receptor involved in immune responses to a variety of inflammatory stimuli (1–3). It is a cofactor of TLRs 2, 3, 4, 7, and 9 in mouse and TLRs 2, 4, and 9 in humans (4) and thus involved in the recognition of a variety of pathogen- or damage-associated molecular patterns. A number of exogenous and endogenous CD14 ligands have been identified, mostly being acylated structural components such as lipopeptides and glycolipids (5–7). Thus, CD14 is a multifunctional, upstream regulator of innate immune function and is therefore an attractive target for directed inhibition of a broad spectrum of inflammatory threats such as sepsis, ischemia reperfusion injury, and trauma- or burn-induced systemic inflammatory response syndrome. Recently, the role of CD14 was highlighted as an essential molecule in TLR4-induced lethal influenza in mice (8).

Abs are being used increasingly in clinical medicine (9–11). IgG is most often the isotype of choice because it has a long serum $t_{1/2}$ and a unique biodistribution owing to neonatal Fc receptor (FcRn) binding (12). Effector functions vary with IgG subclass; depending on the therapeutic strategy, one can aim to induce or avoid them. For target cell killing in cancer therapy, IgG1 is the preferred subclass, because IgG1 binds and activates Fcγ receptors (FcγRs) expressed on macrophages, granulocytes, dendritic cells, and NK cells and activates complement. Consequently, IgG1 exerts effector functions such as Ab-dependent cell cytotoxicity, complement-dependent cytotoxicity (CDC), phagocytosis, and release of immunoregulatory molecules as cytokines (13). For the therapeutic anti-human complement factor 5 (C5) Ab eculizumab (Soliris), however, effector functions are not desired and have been minimized by the use of a hybrid Fc portion, which consists of sequences from human IgG2 and IgG4 to minimize both FcγR binding (IgG2 portion) and complement activation (IgG4 portion) (14, 15).

The effect of neutralizing anti-CD14 Abs has been examined in pig and monkey sepsis models with efficient inhibition of the inflammatory response, but without increased survival (16, 17). A recombinant anti-CD14 Ab IC14 of the human IgG4 subclass, used as single therapy, failed to decrease the inflammatory response consistently in patients suffering from severe sepsis, despite promising anti-inflammatory effects in human low-grade endotoxemia (18, 19). Furthermore, the treatment was associated with reactions that appear to be anaphylaxis. Notably, such IgG-mediated reactions

*Somatic Research Center, Nordland Hospital, Bodø N-8092, Norway; [†]Centre for Immune Regulation, University of Oslo, Oslo N-0027, Norway; [‡]Department of Immunology, Oslo University Hospital Rikshospitalet and University of Oslo, Oslo N-0027, Norway; [§]Department of Biosciences, University of Oslo, Oslo N-0027, Norway; [¶]Faculty of Health Sciences, University of Tromsø, Tromsø N-9037, Norway; [‖]Veterinary Pathology, Infection and Immunity, School of Clinical Veterinary Science, University of Bristol, Bristol BS40 5DU, United Kingdom; and [#]Norwegian University of Science and Technology, Centre of Molecular Inflammation Research, and Department of Cancer Research and Molecular Medicine, Trondheim N-7491, Norway

Received for publication June 21, 2013. Accepted for publication August 11, 2013.

This work was supported by the Northern Norway Regional Health Authority (Grant SFP914-10 to C.L.), the Norwegian Research Council (Grants 179513 to K.G. and 1970 to L.S.H.), the South-Eastern Norway Regional Health Authority (Grant 39375 to J.T.A.), the Odd Fellow Foundation, and the Norwegian Council on Cardiovascular Disease.

Address correspondence and reprint requests to Prof. Tom Eirik Mollnes, Rikshospitalet University Hospital, Rikshospitalet, Oslo NO-0027, Norway. E-mail address: t.e.mollnes@medisin.uio.no

The online version of this article contains supplemental material.

Abbreviations used in this article: CH, H chain C region; MWCO, m.w. cutoff; NIP, 4-hydroxy-3-iodo-5-nitrophenylacetic acid; oriP, origin of replication; pFcRn, porcine FcRn; raNIP, recombinant anti-NIP.

in mouse and humans have been linked to Fcγ receptor (FcγR) binding, and in particular to binding of FcγRIII (20). Abs of the IgG4 subclass bind FcγIII, whereas IgG2 does not (21). One would expect the risk for anaphylactic reactions to be greatly reduced when Abs with the hybrid IgG2/IgG4 Fc portion are used.

We have previously used human and porcine whole blood in ex vivo models of gram-negative bacteria–induced inflammation and observed marked inhibitory effects of anti-CD14, particularly in combination with inhibition of the complement system, on a broad spectrum of inflammatory mediators (22–27). Because the pig is emerging as a nonprimate mammal of choice for preclinical studies of human diseases, including those involving innate immunity and CD14 (17, 28), there is an urgent need for anti-porcine CD14 Abs that do not induce undesired effector functions.

The aim of this study was to construct and characterize such Abs with minimal ability to activate complement and bind to FcγRs. To this end, we have generated recombinant anti-porcine and anti-human CD14 Abs endowed with the IgG2/IgG4 hybrid Fc region. We demonstrate that such novel Abs are unique tools for future studies of CD14 inhibition using porcine in vivo models, and pave the way for human therapy with CD14 inhibition, preferentially in combination with complement inhibition.

Materials and Methods

Abs and inhibitors

Commercial anti-CD14 Abs and isotype controls were purchased at Diatec Monoclonals AS (Oslo, Norway) and AbD Serotec (Kidlington, U.K.) as follows: mouse anti-human CD14 IgG1 clone 18D11 (Diatec), 18D11 IgG1 F(ab)′2 (Diatec), mouse anti-porcine CD14 IgG2b clone Mil2 (Serotec) and FITC-conjugated Mil2 (Serotec), isotype controls mouse IgG1 (Diatec), mouse IgG1 F(ab)′2 (Diatec), mouse IgG2b (Diatec), and FITC-conjugated mouse IgG2b (Serotec). Furthermore, we used the fully humanized anti-C5 IgG2/4 Ab eculizumab (Soliris), purchased from Alexion Pharmaceuticals (Cheshire, CT), as isotype control for recombinant IgG2/4 and humanized anti-CD20 IgG1 Ab rituximab (MabThera) from Roche (Welwyn Garden City, U.K.) as control for ELISA-based binding studies. The rMil2 Ab preparation used in the experiments shown in Figs. 3 and 6 was produced by ExcellGene SA (Monthey, Switzerland). This Ab consists of the same amino acid sequence presented in Supplemental Table I, but was expressed in a CHO cell-expression system. It was pure and free of single chains, as confirmed by SDS-PAGE (not shown).

Goat-anti human IgG κ pooled antisera, HRP-conjugated goat-anti human IgG Fc pooled antisera, HRP-conjugated goat anti-mouse IgG Ab, and PE-conjugated anti-mouse IgG were purchased from Southern Biotech (Birmingham, AL). Mouse monoclonal anti-human IgG2 Ab (clone 3C7) was purchased from Hytest (Turku, Finland).

Endotoxin-free recombinant bacterial OmCI (also known as coversin) (29), a 16.8-kDa protein, was provided by Varleigh Immuno Pharmaceuticals (Jersey, Channel Islands). OmCI has been shown to inhibit complement activation effectively in pigs (30).

Variable gene retrieval and cloning of recombinant anti-CD14 Abs

Original hybridoma cell clones were generated in the laboratories of the coauthors T.E. (18D11) and C.R.S. (Mil2). After brief culture, the cells were harvested and total RNA was extracted using mirVana (Life Technologies, Ambion, Austin, TX). Variable genes were specifically reverse transcribed from 500 ng total RNA using SuperScript II reverse transcriptase and oligonucleotide primers, which were designed to bind downstream of the variable genes in conserved sequences encoding the constant regions of heavy and light chains. After removal of input RNA from the sample by RNaseH digestion (New England Biolabs, Hedfordshire, U.K.), poly dCTP 3′-tailing of the cDNA was performed using rTerminal transferase (Roche Diagnostics, Mannheim, Germany), and fragments containing the variable gene segments were amplified by nested PCR using Phusion DNA polymerase (Finnzymes, Vantaa, Finland) and new sets of primers containing *Bgl*II and MluI restriction sites. The amplicons were inserted in cloning vectors before sequencing analyses. All primers were synthesized by Sigma-Aldrich (Steinheim, Germany; Supplemental Table II).

A well-established protocol (31) was used to subclone the murine variable heavy and variable L chain genes into pLNOH2 and pLNOK expression vectors, respectively. The sequence encoding the human IgG2/4 hybrid constant H chain was consistent with the literature (14) and inserted into pLNOH2. All genes were synthesized by GenScript (Piscataway, NJ). The control Ab specific for a hapten (4-hydroxy-3-iodo-5-nitrophenylacetic acid [NIP]) was also expressed from pLNOH2 and pLNOK (31). Thus, two plasmids were generated for the expression of each of the three recombinant Abs, which target human CD14 (recombinant 18D11, r18D11), porcine CD14 (recombinant Mil2, rMil2), or NIP (recombinant anti-NIP, raNIP). For transfection, plasmid DNA was purified using EndoFree Plasmid Maxi or Mega Kit from Qiagen (Hilden, Germany). Amino acid sequences of the recombinant Abs and related IMGT accession numbers are displayed in Supplemental Table I.

Cell culture

Adherent HEK293-EBNA cells were subcultured at 5% CO_2 and 37°C using DMEM containing 4.5 g/L L-glucose (Lonza, Verviers, Belgium) and substituted with 10% FBS FBS Gold (PAA Laboratories, Pasching, Austria), 4 mM L-glutamine (Lonza), 10,000 U/ml penicillin, and 10,000 μg/ml streptomycin (Lonza). The day before transfection, 4×10^6 cells were seeded in a 75-cm^2 tissue culture flask (Techno Plastic Products, Trasadingen, Switzerland) and grown for an additional 24 h to reach 90% confluency. Cotransfection with light and H chain encoding plasmid DNA in an equimolar ratio was performed in serum-free OptiMEM (Life Technologies, Paisley, U.K.) using Lipofectamine 2000 (Life Technologies, Invitrogen Carlsbad, CA) following the manufactures instructions. Transient expression was performed in a fed-batch procedure with harvest of cell culture supernatant every third day over 12 d. The cells were detached and centrifuged for 5 min at 230 × *g* followed by careful aspiration of the supernatant and immediate resuspension and reseeding of the cells in 12 ml fresh OptiMEM. The supernatant was stored at −20°C until Ab purification. Cell viability and count was monitored throughout subculture and before every harvest using Countess Automated Cell Counter (Life Technologies, Invitrogen).

IgG purification

Concentrators, spin columns, and kits for purification of recombinant Abs and subsequent buffer exchange were purchased from Thermo Scientific, Pierce (Pierce Biotechnology, Rockford, IL). The combined supernatants of each expression culture were centrifuged for 10 min at 1500 × *g* and subsequently filtrated using a sterile vacuum filter system with a 0.22-μm cellulose acetate membrane (Corning Glass Works, Corning, NY). Then, solutions were concentrated using Pierce's concentrators with a 20-kDa m.w. cutoff (MWCO), and OptiMEM was exchanged to sterile PBS using 10 ml Zeba Desalt Spin Columns with a 7-kDa MWCO. The recombinant Abs were purified using an NAb Protein A Plus Spin Kit with a binding capacity of 7 mg IgG per 0.2 ml resin. Ab-containing fractions were combined before buffer exchange to sterile PBS using 2 ml Zeba Desalt Spin Columns with a 7-kDa MWCO and optional upconcentration to 0.5–1 mg/ml using Amicon Ultra 0.5-ml spin columns with a 50-kDa MWCO (Millipore, Carrigtwohill, Ireland). Endotoxin levels in the final batch preparations were less than 0.04 EU/ml, determined using QCL-1000 (Lonza, Walkersville, MD).

Ab expression was monitored using the κ-chain–specific goat-anti human IgG pooled antisera diluted to 1 μg/ml in carbonate buffer as capture and the HRP-conjugated, Fc-specific goat-anti human IgG pooled antisera diluted 1:8000 in PBS for detection (see above).

SDS-PAGE and Western blot

All materials were purchased from Bio-Rad Laboratories AB (Hercules, CA), except where indicated differently. Purified Ab fractions were separated using SDS-PAGE on a Mini-PROTEAN Tetra Cell using Mini-PROTEAN Precast Gels (4–15%) and Tris Glycin SDS buffer. Samples were diluted in 2x Laemmli buffer with or without 5% β-mercaptoethanol. Gels were stained with Biosafe Coomassie G250 following the manufacturer's instructions. Alternatively, proteins were blotted onto a Hybond ECL nitrocellulose membrane (Amersham Pharmacia Biotech, Buckinghamshire, U.K.). After blocking with 5% nonfat dry milk, the membrane was incubated with primary mouse anti-human IgG2 Ab (clone 3C7; 1 μg/ml) and secondary HRP-conjugated goat anti-mouse IgG Ab. Detection of specific bands by ECL was performed using SuperSignal West Dura (Pierce Biotechnology). Images were taken with a ChemiDoc XRS+ system.

CD14 binding in flow cytometry

Fresh human or porcine whole blood was drawn into tubes containing the anticoagulants lepirudin (Refludan; Pharmion, Copenhagen, Denmark) or EDTA, respectively. Blood samples were preincubated for 10 min with Ab, ≤20 μg/ml anti-human CD14 Abs r18D11, 18D11 F(ab)′2 (batch 2068, lot 1383), or isotype controls raNIP and mIgG1 F(ab)′2 (lot 1501), or 100 μg/ml anti-porcine CD14 Abs rMil2, Mil2 (lot 1106), or the isotype controls

for IgG2/4 and mIgG2b, eculizumab (Soliris) and mIgG2b (lot 1631), respectively. Endotoxin-free Dulbecco phosphate buffered saline, PBS (Sigma-Aldrich), was used for diluting the Abs. Subsequently, blood samples were incubated for another 15 min in the presence of detection Ab, 10 μg/ml 18D11 (batch 719, lot 3110) or 150 μg/ml FITC-conjugated Mil2 (batch 1107). Their binding was detected either by using a secondary PE-conjugated anti-mouse IgG or through direct FITC fluorescence. Erythrocytes were lysed using FACS Lysing solution (BD Biosciences, Franklin Lakes, NJ; human blood) or a solution of 0.16 M ammonium chloride, 10 mM sodium bicarbonate, 0.12 mM EDTA (Tritiplex III) and 0.04% (v/v) paraformaldehyde (porcine blood). In subsequent flow cytometry analyses, human monocyte and porcine granulocyte populations were selected based on the forward scatter–side scatter dot plot, and CD14 binding was recorded as mean or median fluorescence intensity, respectively. In contrast to humans, porcine CD14 is constitutively expressed on mature granulocytes (32, 33). Fluorescence intensities in the presence of the fluorescently labeled Abs only were set to 100%. Flow cytometry analyses on human samples were performed using an LSRII and FACSDiva software version 5.0.3; porcine samples were analyzed on a FACSCalibur using Cell Quest Pro version 5.2.1 for data acquisition (all from BD Biosciences).

Construction, production, and purification of recombinant soluble FcRn and FcγR variants

The vector containing a truncated version of human FcRn (hFcRn) H chain cDNA encoding the three ectodomains (α1–α3) genetically fused to a cDNA encoding the *Schistosoma japonicum* GST has been described earlier (34). The vector-denoted pcDNA3-hFcRn-GST-hβ2m– origin of replication (oriP) also contains a cDNA encoding human β2-microglobulin and the EBV oriP. A truncated cDNA segment encoding the extracellular domains of porcine FcRn (pFcRn) was synthesized by Genscript and subcloned into the pcDNA3-GST-hβ2m-oriP vector using the restriction sites *Eco*RI and *Xho*I. Vectors encoding the ectodomains of human FcγRI, FcγRIIa, FcγRIIb, FcγRIIIa, and FcγRIIIb fused to GST have been described previously (34, 35). All recombinant soluble receptors were produced by transient transfection of HEK293-EBNA cells, and secreted receptors were purified using a GSTrap column as described previously (34).

ELISA for C1q, FcγR, and FcRn binding

Ninety-six–well plates (Nunc, Roskilde, Denmark) were coated with serial dilution of the Abs (6.0–0.09 μg/ml) and incubated overnight at 4°C followed by washing three times with PBS/Tween (pH 7.4). The wells were blocked with 4% skimmed milk (Neogen Europe, Auchincruive, U.K.) for 1 h at room temperature and then washed in PBS/Tween (pH 6.0). Purified hFcRn-GST or pFcRn-GST (1 μg/ml) were diluted in 4% skimmed milk in PBS/Tween (pH 6.0) and preincubated with an HRP-conjugated anti-GST Ab (GE Healthcare U.K., Buckinghamshire, U.K.) diluted 1:5000 and added to the wells. The plates were incubated for 1 h at room temperature and washed with PBS/Tween (pH 6.0). Bound receptor was detected by adding 100 μl of 3,3′,5,5′-tetramethylbenzidine substrate (Calbiochem-Novabiochem, Nottingham, U.K.). The absorbance was measured at 450 nm using a Sunrise TECAN spectrophotometer. The assay described above was also performed using PBS/Tween (pH 7.4) in all steps. The same setup was used with GST-fused versions of hFcγRI, hFcγRIIa (allotype His131), hFcγRIIb, hFcγRIIIa (allotype Val158), and hFcγRIIIb (1 μg/ml each). In addition, a biotinylated human C1q (hC1q; 4 μg/ml) preparation was incubated with the Abs and detected using ALP-conjugated streptavidin (GE Healthcare). Absorbance was measured at 405 nm.

Whole blood ex vivo model of inflammation

The whole blood model has been described in detail previously (36). Fresh human venous or porcine arterial blood was drawn directly into tubes containing the anticoagulant lepirudin (Pharmion) at a final concentration of 50 μg/ml. In 1.8-ml Cryo Tube vials (Nunc, Roskilde, Denmark), the blood was preincubated with up to 20 μg/ml anti-human CD14 (r18D11 or 18D11), or 50 μg/ml anti-porcine CD14 (rMil2 or Mil2) at 37°C for 10 min prior to an additional 2-h incubation in the presence of 100 ng/ml ultrapure LPS from *Escherichia coli* O111:B4 (InvivoGen, San Diego, CA) for human blood or 1×10^5/ml heat-inactivated *E. coli* (strain LE392, ATCC33572) for porcine blood. As negative controls, PBS with $MgCl_2$ and $CaCl_2$ (Sigma-Aldrich) and isotype controls were used. Adverse effects were tested using nonactivated whole blood samples. After the addition of 10 mM (human) or 20 mM (porcine) EDTA, plasma was gained by 15 min centrifugation at 3220 × *g* and 4°C. Levels of TNF, IL-6, and IL-1β in human plasma were determined using Bioplex technology (Bio-Rad Laboratories AB). Levels of TNF, IL-1β, and IL-8 in porcine plasma were determined using ELISA (Quantikine, R&D Systems, Minneapolis, MN). Platelet count was quantified by impedance using a CELL-DYN Sapphire hematology analyzer (Abbott Laboratories, Abbott Park, IL).

Effect of rMil2 combined with the complement C5 inhibitor OmCI on cytokine production in porcine whole blood ex vivo

Whole blood was incubated with 1×10^6 *E. coli* per milliliter for 2 h at 37°C in the absence or presence of inhibitors and controls. TNF, IL-1β, and IL-8 blood was analyzed as described above.

Effect of rMil2 combined with the complement C5 inhibitor OmCI on leukocyte tissue factor expression

For analysis of leukocyte expression of tissue factor (TF), porcine whole blood was incubated with 5×10^6 *E. coli* per milliliter in the absence or presence of inhibitors and controls. After incubation, the tubes were put on ice, citrate was added to stop the activation, and the samples further analyzed by flow cytometry. One sample was split into two tubes and stained with sheep anti-human TF (Affinity Biologicals, Ancaster, Canada) and control sheep IgG (Sigma-Aldrich, Saint Louis, MO), respectively. All samples were incubated for 30 min at 4°C, and red cells were lysed and centrifuged at 300 × *g* for 5 min at 4°C. The cells were washed with PBS (0.1% BSA; BioTest, Dreieich, Germany). Samples were further stained with rabbit anti-sheep IgG-PE conjugate (Santa Cruz Biotechnology, Dallas, TX) for an additional 30 min at 4°C and then washed twice as described above. The cells were resuspended in PBS (0.1% BSA) before they were run at the flow cytometer (FACSCalibur; Becton Dickinson, Franklin Lakes, NJ). Granulocytes were gated in a forward scatter–side scatter dot plot, and TF expression was given as median fluorescence intensity.

In vivo application of anti-porcine CD14 Abs

Norwegian domestic piglets (*Sus scrofa domesticus*, outbred stock) with a weight of 2.2 kg were isolated at the day of intervention. Anesthesia was induced with 5% sevoflurane in a mixture of air and oxygen until sleep. After establishment of an i.v. line, the piglets received fentanyl (15–20 μg/kg) were tracheotomized in the supine position, and a microcuffed endotracheal tube from Kimberly-Clark (Roswell, GA) with inner diameter of 4 mm was inserted. Maintenance anesthesia was provided with an infusion of fentanyl (50 μg/kg/h, and isoflurane 1–2% in oxygen-enriched air administered from a Leon plus ventilator from Heinen and Loevenstein (Bad Ems, Germany). An artery line was inserted in the right or left carotid artery for blood sampling during the experiments and for continuous measurement of mean artery pressure. The piglets were monitored with electrocardiography and pulse oximetry. Ventilator settings were adjusted to maintain 7.40 pH and oxygen saturation above 96%. Hemodynamic parameters were collected using ICUpilot software, CMA Microdialysis (Stockholm, Sweden) every 30 s. To compensate for hydration needs, the animals received a background infusion of isotonic sodium glucose solution, Salidex (Braun Medical A/S, Vestskogen, Norway) at 10 ml/kg/h.

To compare the effect of the Mil2 and the rMil2 on healthy piglets, increasing amounts of a stock solution of 1 mg/ml rMil2 or Mil2 (batch 1106) were injected i.v. into two piglets at indicated times to a maximum dose of 5.36 mg/kg, and arterial blood samples were collected, in tubes containing the anticoagulants EDTA or citrate. To investigate the biological effect of rMIL2 on the inflammatory response, two piglets underwent the *E. coli* sepsis regimen as described previously (17). One control piglet was gives saline, and one piglet was given a bolus dose of 5 mg/kg rMil2 before infusion of the bacteria.

Data presentation and statistics

All graphs were generated and statistical analyses were performed using GraphPad Prism version 5.03 from GraphPad Software (San Diego, CA). If not indicated differently, arithmetic mean values and SEM are displayed. Statistical significance was calculated using ANOVA and Tukey, Dunnett, or Bonferroni posttest analysis for subgroup comparison as indicated in the figure legends. Student *t* test was used to compare combined inhibition of anti-CD14 and OmCI compared with the two single inhibitions.

Ethics

The study was approved by the Norwegian Government Regional Committee for Medical Research and by the Norwegian Animal Research Authority.

Results

Cloning and expression of recombinant anti-CD14 Abs

Recombinant anti-porcine CD14 (rMil2) and anti-human CD14 (r18D11) Abs were generated, as both mouse human chimeras with

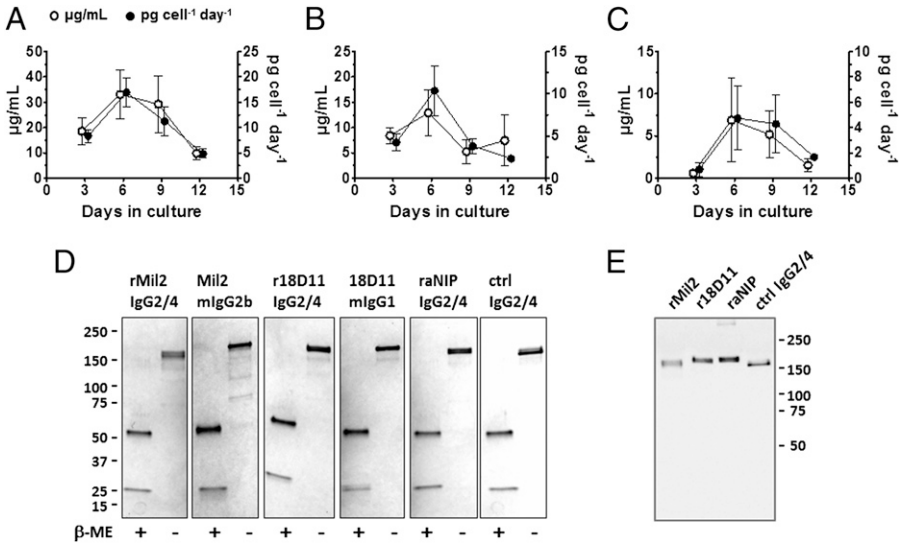

FIGURE 1. Expression of recombinant IgG2/4 hybrid Abs. (**A**–**C**) The Ab concentration in cell culture supernatant (µg/ml; ○) and the Ab production rate (pg/cell/day; ●) during a fed-batch expression period of 12 d were determined with ELISA. Data are given as mean and SEM for rMil2 (A; n = 12), r18D11 (B; n = 5) and raNIP (C; n = 2). (**D**) Five hundred nanograms of each purified Ab was subjected to either reducing or nonreducing SDS-PAGE and stained with Coomassie Blue. IgG2/4 isotype controls raNIP and anti-human C5 Ab eculizumab (ctrl IgG2/4) were included. (**E**) The same samples (10 ng) were subjected to nonreducing SDS-PAGE and immunoblotting using an Ab specific for the human IgG2 hinge region.

murine variable and human constant regions (Supplemental Table I). For both region, the H chain C region (CH) was chosen such that the CH1 and hinge regions were from IgG2, whereas the CH2 and CH3 domains were from IgG4. The variable genes encoding the Ab specificities are identical to those of the original murine clones 18D11 and Mil2 (Supplemental Table I). raNIP with the same C region was also generated and included as isotype control in further studies.

All Abs were readily expressed in adherent HEK293-EBNA cells after transient transfection, although at different levels. During expression under serum-free conditions, ~ 20 µg/ml rMil2 was produced, while r18D11 and raNIP were produced at 4-8 µg/ml (Fig. 1A-C). For rMil2, production reached a maximum of 15 pg/cell/d between days 6 and 9 (Fig. 1A). The recombinant Abs were purified from the cell culture supernatant, subjected to re-

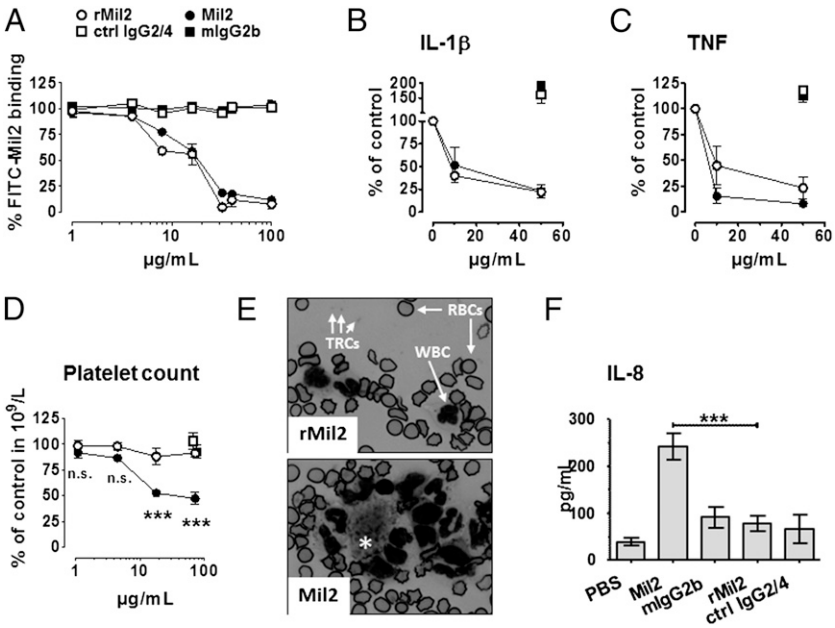

FIGURE 2. Functional characterization of anti-porcine CD14 Ab rMil2. (**A**) Whole porcine blood was incubated with 150 µg/ml FITC-conjugated Mil2 (FITC-Mil2) and increasing concentrations of unlabeled rMil2 (○), control IgG2/4 (eculizumab) (□), the original clone Mil2 (●) or mIgG2b isotype control (■). Remaining FITC-Mil2 binding to the granulocyte population was recorded as median fluorescence intensity of using flow cytometry. Fluorescence intensity in presence of FITC-Mil2 alone was set to 100%. (**B** and **C**) Release of the proinflammatory cytokines IL-1β (B) and TNF (C) from porcine whole blood induced with 1×10^5/ml *E. coli* strain LE392 in presence of increasing concentrations of rMil2 (○), Mil2 (●), control IgG2/4 (□), or mIgG2b (■). After 120 min incubation, plasma cytokine levels were determined with ELISA, and those measured in absence of any exogenous Ab were set to 100%. (**D**) Porcine whole blood was incubated with increasing concentrations of rMil2 or Mil2, or ctrl IgG2/4 or mIgG2b isotype controls (up to 71.4 µg/ml). Platelet counts were determined by flow cytometry in routine analysis. Significance for differences in values for rMil2 (○) and Mil2 (●) was calculated by two-way ANOVA and Bonferroni post test (***$p < 0.001$). (**E**) Blood slides from samples containing 71.4 µg/ml rMil2 or Mil2 were stained with nuclear stain and investigated by light microscopy. Pictures were taken at a 1000-fold magnification. WBCs, RBCs, and platelets (thrombocytes [TRCs) are indicated by arrows. The single asterisk in the picture for Mil2 indicates a platelet aggregate with surrounding leukocytes that was not observed in rMil2-treated blood. (**F**) Porcine whole blood was incubated with 50 µg/ml rMil2 (○), Mil2 (●), control IgG2/4 (□) or mIgG2b (■). After 120 min, plasma levels of IL-8 were measured using ELISA. Data are given as mean and SEM for (A, D, and F) (all n = 3) and as mean and range for (B) and (C) (n = 2). Significance for difference in values for Mil2 and rMil2 (***$p < 0.001$) was calculated by one-way ANOVA and Tukey post tests. n.s., not significant.

ducing and nonreducing SDS-PAGE, and compared with commercially available batches of their original murine clones (Fig. 1D). The recombinant Abs were also detected by an anti-human IgG2 hinge Ab after Western blotting (Fig. 1E).

Functional characterization of the recombinant anti-porcine CD14 Ab rMil2

Whole blood from healthy pigs was used to study Ag-binding and CD14-blocking effects of the recombinant anti-porcine CD14 Ab rMil2. rMil2 effectively bound to and displaced the original clone, Mil2, from $CD14^+$ granulocytes (Fig. 2A). Both rMil2 and Mil2 competed equally well with FITC-conjugated Mil2 in binding to CD14, and they blocked nearly 50% of the binding sites at 15 μg/ml. At this concentration, direct binding of rMil2 to porcine granulocytes was saturated (not shown).

Furthermore, rMil2 effectively inhibited the proinflammatory cytokine response in whole blood induced by 1×10^5 cells/ml heat-inactivated *E. coli* (Fig. 2B, 2C). Therefore, it was as effective as Mil2 in the block of IL-1β release, and slightly less inhibitory on TNF release. In the presence of 10 μg/ml and 50 μg/ml of either Ab, IL-1β and TNF plasma levels were reduced by at least 75% and 50%, respectively.

Next, we tested for unwanted IgG-Fc mediated effects of rMil2 and Mil2 in the absence of inflammatory stimuli (Fig. 2D–F). We observed a dose-dependent drop in platelet counts for Mil2 (Fig. 2D). This highly significant drop was most likely the result of platelet activation and aggregation, and platelet aggregates surrounded by leukocytes were observed in blood slides from the same samples (Fig. 2E). In addition, Mil2 induced a strong spontaneous IL-8 release (Fig. 2F). Neither IL-8 secretion nor platelet drop nor aggregation were observed in the presence of rMil2. None of the Abs induced significant complement activation, measured as terminal C5b-9 complement complex formation (not shown).

Effect of rMil2 in combination with the complement C5 inhibitor OmCI on the inflammatory response

Based on recent promising data supporting a combined inhibition of CD14 and the complement system as a therapeutic approach for inflammatory conditions (37), we investigated the effect of the original Mil2 and the rMil2 alone and in combination with the complement C5 inhibitor OmCI. Porcine whole blood was incubated with *E. coli* and the cytokine response (TNF, IL-1β, IL-8) and expression of granulocyte TF were studied (Fig. 3).

TNF release was significantly reduced by a single treatment with OmCI and original Mil2 ($p < 0.01$), with rMil2, and with OmCI combined with either of the Mil2 Abs ($p < 0.001$; Fig. 3A). The combination of OmCI and rMil2 was the most effective inhibitory regimen (81% inhibition as compared with *E. coli*; $p < 0.001$) and significantly more effective than OmCI or rMIL2 alone ($p = 0.001$ and $p = 0.004$, respectively).

IL-1β release was not significantly reduced by a single treatment with OmCI or original Mil2, but rMil2 alone and OmCI combined with either Mil2 Abs significantly reduced the production ($p < 0.05$; Fig. 3B). The combination of OmCI and rMil2 was the most effective inhibitory regimen (94% inhibition as compared with *E. coli*; $p < 0.01$) and significantly more effective than OmCI or rMil2 alone ($p = 0.002$ and $p = 0.019$, respectively).

IL-8 release was significantly reduced to almost baseline by OmCI alone ($p < 0.05$), whereas original Mil2 markedly enhanced the release (Fig. 3C), consistent with the adverse effects of IL-8 by the original Ab observed previously (Fig. 2F). The inhibition seen with rMil2 alone seemed to be substantial, but did not reach statistical significance, presumably because of type II error. Notably, the combination of OmCI and rMil2 was again the most effective

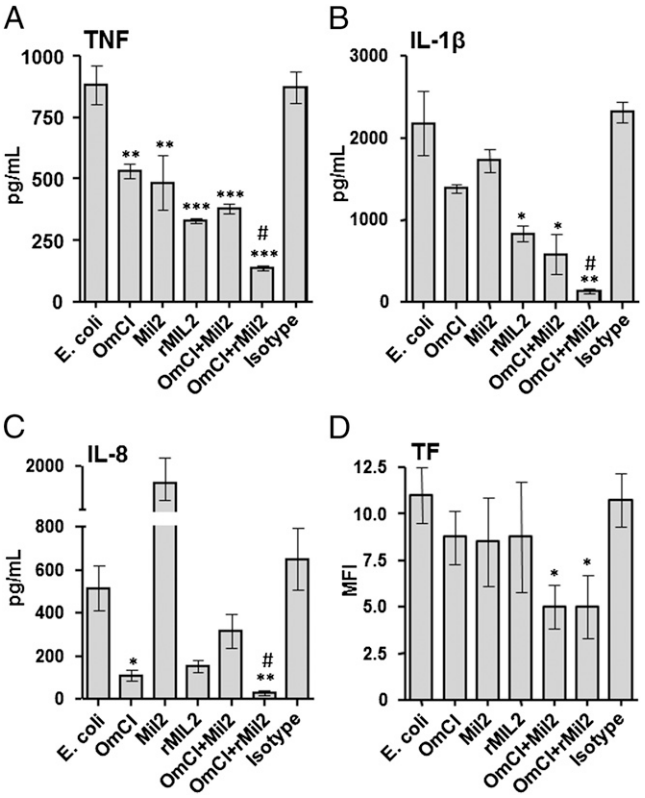

FIGURE 3. Effect of rMil2 in combination with C5-inhibitor OmCI on the inflammatory response in porcine blood in vitro. Porcine whole blood was incubated with *E. coli* in the presence of PBS (*E. coli*), the complement C5 inhibitor OmCI (0.32 μM), original anti-CD14 Ab Mil2 (25 μg/ml), recombinant anti-CD14 Ab rMil2 (25 μg/ml), the combination of OmCI and the two Mil2 Abs, or an isotype control Ab. Plasma was analyzed for cytokines. (**A**) TNF. (**B**) IL-1β. (**C**) IL-8. (**D**) TF expression on granulocytes was measured by flow cytometry and expressed as median fluorescence intensity (MFI). Results are shown as mean ± SEM of four to eight experiments. #Statistical significance between combined inhibition versus the two single inhibitions (for detailed *p* values, see *Results*). *Statistical significance as compared with *E. coli* alone (left column). *$p < 0.05$, **$p < 0.01$, ***$p < 0.001$.

inhibitory regimen (94% inhibition as compared with *E. coli*; $p < 0.01$) and significantly more effective than OmCI or rMil2 alone ($p = 0.033$ and $p = 0.008$, respectively).

TF, as expressed by neutrophils, was significantly reduced only by the combined inhibition of OmCI and the two anti-CD14 Abs (Fig. 3D; $p < 0.05$), rMil2 being similarly effective as the original Mil2.

Functional characterization of recombinant anti-human CD14 r18D11

The recombinant anti-human CD14 Ab, r18D11, was tested with respect to Ag binding and inhibition of CD14-mediated cytokine release. It dose-dependently outcompeted the binding of the original clone, 18D11, to CD14-positive sites on human monocytes (Fig. 4A). The same was observed with a F(ab)′2 fragment of the original clone. This indicates that the Abs bind to the same epitope, as expected. Equimolar amounts of r18D11 (10 μg/ml) displaced 50% of 18D11 from its binding sites. The lower competitive activity of 10 μg/ml r18D11 compared with 10 μg/ml of the F(ab)′2 fragment of the murine clone is due to difference in molarities. Neither raNIP nor a control F(ab)′2 fragment bound human CD14 (Fig. 4A).

Furthermore, both 18D11 and r18D11 inhibited *E. coli* ultrapure LPS-induced release of the proinflammatory cytokines IL-1β, TNF, and IL-6 in human whole blood, in a dose-dependent manner

(Fig. 4B–D). Maximum inhibitory effects were reached at an Ab concentration of 10 μg/ml, at which the recombinant clone was as effective as the original clone. Again, neither raNIP nor control mIgG1 inhibited LPS-induced cytokine release.

Induction of unwanted effects, such as complement activation and oxidative burst, was tested using nonstimulated human whole blood supplemented with 10 μg/ml Ab. The original clone 18D11, r18D11, and raNIP induced the same low level of complement activation, whereas the F(ab)′2 fragment of 18D11 and a mIgG1 isotype control did not (not shown). Monocyte oxidative burst, however, was significantly induced by the original 18D11 clone, comparable to that of the positive fMPL control (Fig. 4E). Notably, r18D11 did not induce significant oxidative burst, and was comparable with the $F(ab')_2$ 18D11, the isotype IgG1 control and the IgG2/4 chimeric negative control raNIP (Fig. 4E).

Binding of rMil2 and r18D11 to complement component C1q and Fc receptors

To test further for potential activation of the classical complement pathway and FcR, binding of the recombinant IgG2/4 Abs to C1q and human FcγRs was measured by ELISA (Fig. 5). Importantly, none of them bound to C1q, whereas the positive control, a human IgG1 (rituximab), did so in a dose-dependent manner (Fig. 5A). The same was observed for all tested FcγRs, except for FcγRIIa allotype His131 (Fig. 5C). Here, the recombinant Abs bound to the receptor, though less than human IgG1.

Furthermore, we tested for binding to the FcRn, which plays a crucial role in IgG $t_{1/2}$ regulation and biodistribution. Recombinant IgG2/4 Abs bound both human and porcine FcRn receptors in vitro with dose responses comparable to those for the positive controls, human IgG1, or a porcine IgG pool (Figs. 5G–K). In accordance with the reported pH dependency, both the human and porcine FcRn bound their IgG ligands at an acidic pH ($<$ pH 6.0), whereas binding of IgG at physiologic pH ($\sim$ pH 7.4) was negligible. Binding occurs at the CH2 and CH3 domains of the Fc region, with amino acid 435 (His435 in IgG2) being a key contact residue (12).

In vivo adverse effects induced by anti-porcine CD14 Ab Mil2 are not observed after rMil2 injection in a pig

Intravenous bolus injections of Mil2 to pigs have been observed to disturb the porcine hemodynamics by causing severe peripheral vasodilatation, increase in heart rate, drop in systemic arterial pressure and loss of platelets, together interpreted as reactions that appeared to be anaphylaxis (E.B. Thorgersen, A. Barratt-Due, E.W. Nielsen, and T.E. Mollnes, unpublished observations). Mil2 and rMil2 were therefore compared for induction of these adverse effects in vivo using Norwegian domestic piglets (Fig. 6A–D). In two piglets, a total of 5.36 mg/kg Mil2 or rMil2 were injected as increasing dose over a period of 45 min (Fig. 6A). In vivo binding of Mil2 and rMil2 to porcine CD14 was demonstrated by the blocked binding of FITC-conjugated Mil2 to CD14-positive granulocytes in blood samples collected during infusion. FITC-conjugated Mil2 was added to the blood samples immediately preceding flow cytometry analyses (Fig. 6B). At a total dose of 1.12 mg/kg, which was reached after 20 min, more than 50% of the available cell-bound CD14 was saturated.

Hemodynamic readouts were recorded. Injection of Mil2, but not rMil2, caused an increase in heart rate after 10 min, at which time a total of 0.32 mg/kg Ab had been given (Fig. 6C). For Mil2, the heart rate reached its maximum of ~300 beats/min during the next 5 min and then slowly fell to baseline. Mil2 injection also caused a reversible drop in mean arterial blood pressure, which again was not seen for rMil2 (not shown). Finally, Mil2 injection induced a gradual depletion of platelets, whereas rMil2 did not affect platelet counts (Fig. 6D). The loss of free platelets in the presence of Mil2 could also be visualized on blood slides from the same blood samples (not shown). Thus, none of the adverse effects observed in vivo with Mil2 were observed with rMil2.

In vivo cytokine response induced by E. coli *was abolished by rMil2*

The biologic effect of rMil2 was then investigated. rMil2 was given as a bolus dose to a piglet, and the leukocyte expression of CD14 before and after this bolus was measured using fluorescence-labeled

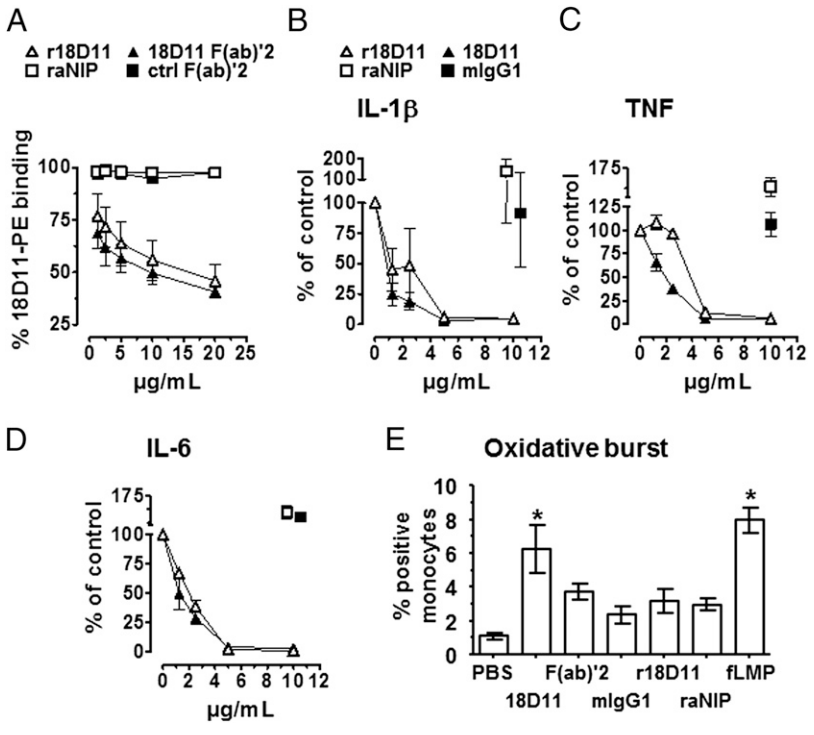

FIGURE 4. Functional characterization of anti-human CD14 Ab r18D11. (**A**) Binding of increasing concentrations of r18D11 (△), raNIP (□), 18D11 F(ab)′2 (▲) or a control F(ab)′2 (■) to monocytes was determined by the ability of the Abs to displace 10 μg/ml of the original clone 18D11 mIgG1 from its CD14 binding site in human whole blood. Mean fluorescence intensity derived from a PE-conjugated anti-mouse IgG Ab was measured using flow cytometry. Fluorescence intensity in presence of original clone 18D11 alone was set to 100%. (**B–D**) Release of the proinflammatory cytokines IL-1β (B), TNF (C), and IL-6 (D) from human whole blood was induced with 100 ng/ml ultrapure LPS from *E. coli* O111:B4 in the presence of increasing concentrations of r18D11 (△) or the original clone 18D11 (▲). raNIP (□) and mIgG1 isotype control (■) (10 μg/ml) served as negative controls. (**E**) Monocyte oxidative burst was measured with flow cytometry after adding the different Ab preparations to human whole blood. Data are given as mean and SEM ($n = 3$ independent experiments). *$p < 0.05$ as compared with the negative PBS control.

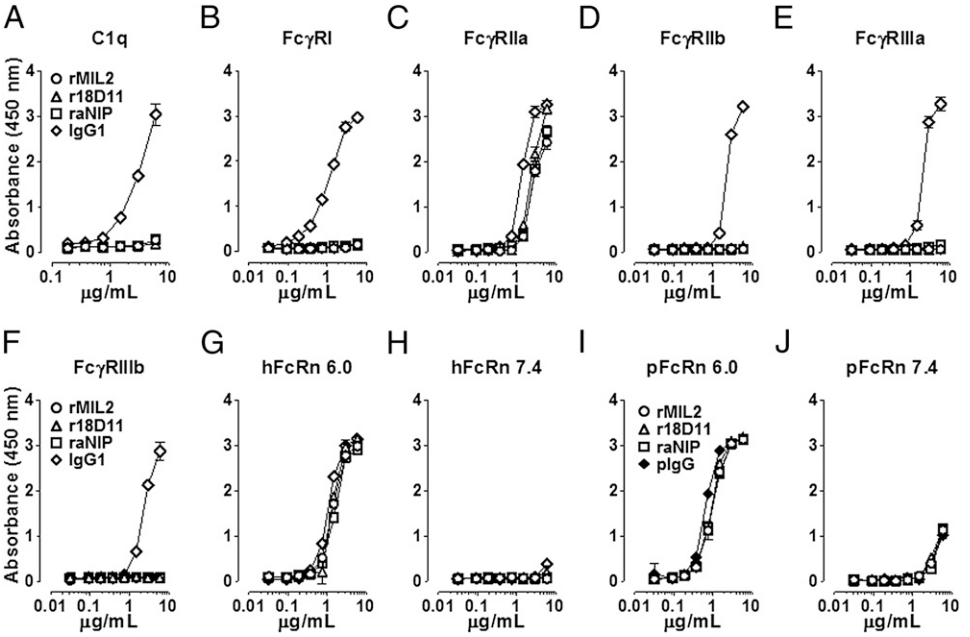

FIGURE 5. In vitro binding of recombinant IgG2/4 hybrid Abs to complement and Fc-receptors. Increasing concentrations of rMil2 (○), r18D11 (△) or raNIP (□) were incubated with (**A**) immobilized human C1q, (**B**) the human Fcγ receptors FcγRI, (**C**) FcγRIIa (allotype His131), (**D**) FcγRIIb, (**E**) FcγRIIIa (allotype Val158), (**F**) FcγRIIIb, and (**G**, **H**) human (hFcRn) or (**I**, **J**) porcine FcRn (pFcRn) at acidic (pH 6.0) and neutral pH (pH 7.4). Human IgG1 (◇) (A–H) or porcine IgG (pIgG; ♦) (I, J) served as positive controls. Binding was measured as absorbance at 450 nm. Data are given as mean and SD (n = 3 independent experiments).

rMIL in flow cytometry. A reduction in CD14 expression by 94% was observed after the bolus of rMIL2 was given, consistent with a virtually complete saturation of CD14 by rMIL2 in vivo (Fig. 6E). Furthermore, rMil2 virtually abolished the *E. coli*–induced cytokine response (Fig. 6F–I). TNF, IL-1β, IL-6, and IL-8 were reduced by 71%, 89%, 88%, and 100%, respectively (area under the curve).

Discussion

In this study, we have generated and intensively tested a recombinant anti-porcine CD14 IgG2/4 Ab (rMil2), which showed to be functional with respect to neutralization of LPS-induced cytokine production and free of undesired Fc-mediated effects. Our data demonstrate that rMil2 can be used for in vivo therapeutic intervention in pig models of inflammation and, thus, constitutes a valuable tool for future studies of in vivo CD14 function, in particular of its crosstalk with complement, since we showed a substantial additional effect by combining rMil2 with the C5 inhibitor, as compared with their single effects.

Blocking human CD14 with the mouse monoclonal anti-CD14 Ab clone 18D11 (F(ab)′2 fragment has been a powerful inter-

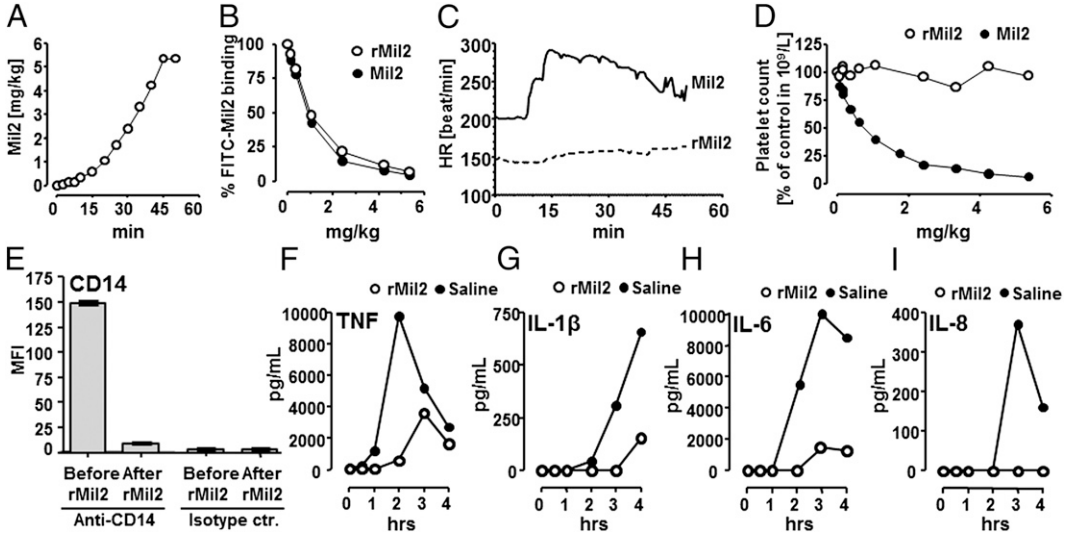

FIGURE 6. In vivo application of anti-porcine CD14 Abs Mil2 and rMil2. Healthy newborn piglets (**A**–**D**) were infused i.v. with increasing amounts of the original clone Mil2 (n = 1) or rMil2 (n = 1) and observed for 50 min. (A) After initial small doses within the first 10 min, Mil2 or rMil2 were given every 5 min for an additional 35 min. After 45 min, a maximum final concentration of 5.36 mg/kg was reached. (B) Saturation of endogenous CD14 binding sites as a function of rMil2 (○) or Mil2 (●) concentration was measured by flow cytometry. Blood samples were incubated with 150 µg/ml FITC-conjugated Mil2, the porcine granulocyte population was selected, and the median fluorescence intensity for bound FITC-Mil2 was recorded. Fluorescence intensity in the absence of nonconjugated anti-CD14 (time point zero) was set to 100%. (C) The heart rate (HR) was recorded in real time throughout the experiments. (D) Blood platelet counts are given as a function of rMil2 (○) or Mil2 (●) concentration. They were corrected for actual hematocrit levels that reflect blood dilution caused by sampling and reconstitution. Levels in the absence of anti-CD14 Ab were set to 100%. Two piglets underwent *E. coli* sepsis (**E**–**I**). One piglet was injected with a bolus dose of rMil2 before i.v. infusion with bacteria and one received saline as control. Expression of leukocyte CD14 was measured before and after rMil2 injection (Fig. 6E). Cytokine release was measured during the 4-h observation period (Fig. 6F–I) comparing saline (●) with rMil2 (○). Anti-CD14, Fluorescence-labeled rMIL2; Islotype ctr, the isotype control for rMIL2.

vention in ex vivo inflammatory models using exogenous danger ligands such as gram-negative bacteria or endogenous danger ligands like meconium (22, 23, 26, 27, 38, 39). In the current study, we have generated a recombinant anti-human CD14 IgG2/4 Ab (r18D11) that blocked CD14-mediated inflammatory responses in a human whole blood model of inflammation, was virtually inert with respect to Fc-mediated binding to complement and FcγRs, and induced no oxidative burst (Figs. 4 and 5). Thus, r18D11 constitutes a highly promising lead for future anti-inflammatory drug engineering and therapeutic intervention.

To study the many roles of CD14 in vivo, pigs are emerging as a valuable test model system. We provide a recombinant anti-porcine CD14 IgG2/4 Ab—rMil2. The original clone Mil2 from which rMil2 is derived has already been used as intervention in porcine sepsis (17). Despite the fact that the application of Mil2 was efficient in reducing the inflammatory response, its bolus application was hampered by the induction of an initial reaction appearing to be anaphylaxis and had a clear limitation for further study. In this study, we show that Mil2 induces unwanted IL-8 release in vitro (Fig. 2) and platelet activation both in vitro and in vivo (Figs. 2 and 6). The latter was accompanied with hemodynamic changes, including decreased arterial blood pressure and increased heart rate. Importantly, we document that none of these effects were induced when rMil2 was used instead, indicating a major step forward with respect to CD14 inhibition in porcine models of relevance to human disease. Finally, we showed that the biologic activity of rMil2 was preserved, as compared with the original Mil2, by blocking leukocyte CD14 and by abolishing *E. coli*–induced cytokine production in vivo. The effect of anti-DC14 on the growth of *E. coli* was not studied. We have, however, shown previously that Mil2 does not affect *E. coli* survival in whole pig blood, in contrast to a complement inhibitor, that increased bacterial survival (25).

IgG infusion-related in vivo reactions that appear to be anaphylaxis, as well as FcγR– Ab-dependent cell cytotoxicity or complement-dependent mediated cytotoxicity, are unwanted events in anti-CD14 based inflammatory therapeutic strategy, where maintenance of homeostasis is the main concern. Now, recombinant anti-CD14 IgG2/4 Abs with minimum Fc-mediated effector functions are available. Of the human IgG subclasses, IgG2 and IgG4 exert the least FcγR binding and complement fixation activities, respectively (21, 40, 41). As expected, the combination of the two subclasses in a human IgG2/4 subclass hybrid abolished binding to complement and any all FcγRs, except FcγRIIa (allotype His131), a low-affinity activating FcγR (Fig. 5). All conventional FcγRs bind their Fc ligands at a site that involves the lower hinge region and the two CH2 domains (42, 43). The recombinant IgG2/4 CH hybrid Abs carry sequences from the human IgG2 subclass in the lower hinge, and all FcγR contact residues in the CH2 domain that were derived from IgG4 are identical to those found in IgG2 (43). Thus, our data are consistent with the fact that FcγRIIa (allotype His131) is the only FcγR that binds IgG2, and thus the IgG2/4 subclass hybrid, with reasonable affinity (21). Importantly, pigs are not known to express FcγRIIa, and the homology between other human and pig FcγRs is more than 60% (44–46). For example, the most important residues in FcγRIIIa for IgG binding, Trp87 and Trp110, are conserved between the pig and human receptors. FcγRIII has been shown to play a key role in IgG mediated anaphylaxis (20), but is bound only weakly by human IgG2 (21). It is, therefore, not surprising that rMil2 with its IgG2/4 hybrid C region does not induce an anaphylactic reaction in pigs.

Human IgG is both readily bound and taken up by pig cells expressing porcine FcRn (47). FcRn regulates the serum $t_{1/2}$ of Abs by a recycling mechanism that requires pH dependent binding (48). In this study, we provide evidence that the human IgG2/4 subclass hybrid Abs bind porcine FcRn in such a pH-dependent manner. This evidence will contribute further to the successful use of Abs with human constant regions in pig.

The exact binding sites of 18D11 and Mil2, and thus of r18D11 and rMil2, on human and porcine CD14 are still not defined. However, as they block CD14 function, it is likely that they bind to either the N-terminal LPS-binding pocket of CD14 or parts of the LPS-signaling motif. Importantly, the hydrophobic binding pocket can also accommodate other acylated endogenous and exogenous ligands of CD14 and TLRs (49–51). Therefore anti-CD14 Abs, like r18D11 and rMil2, may affect pattern recognition signaling upon a wide range of threats, being more efficient than, for example, LPS mimics.

Recently, intensive cross talk has been described for TLR signaling and the complement system, which itself is associated with a plethora of acute and chronic inflammatory disorders (52, 53). This functional interplay has been recognized as an important regulatory mechanism to control both innate and adaptive immune responses (reviewed in Refs. 54–56), and combined inhibition of CD14 and complement has been suggested as an effective therapeutic approach in conditions associated with detrimental activation of the innate immune system (57, 58). We recently showed that combined inhibition on CD14, using the original clone Mil2, and the complement inhibitor OmCI, reduces inflammation, hemostatic disturbances and improved hemodynamics in a porcine model of *E. coli* sepsis (37). These results were obtained despite the adverse effects seen with the original clone Mil2. In this study, we show that rMil2 combined with the complement C5 inhibitor OmCI efficiently attenuates the *E. coli*–induced cytokine response and TF expression in porcine whole blood without any adverse effects (Fig. 3).

The anti-CD14 Abs reported in this study would be particularly valuable tools for future in vivo studies to explore the combined inhibition of CD14 and complement as a therapeutic approach for inflammatory diseases in the future.

Acknowledgments

We thank the routine laboratories of the medical chemistry department at Oslo University Hospital Rikshospitalet for hematology analyses and Margareta Nilsson for performing porcine cytokine analyses.

Disclosures

The authors have no financial conflicts of interest.

References

1. Wright, S. D., R. A. Ramos, P. S. Tobias, R. J. Ulevitch, and J. C. Mathison. 1990. CD14, a receptor for complexes of lipopolysaccharide (LPS) and LPS binding protein. *Science* 249: 1431–1433.
2. Ulevitch, R. J., and P. S. Tobias. 1995. Receptor-dependent mechanisms of cell stimulation by bacterial endotoxin. *Annu. Rev. Immunol.* 13: 437–457.
3. Jersmann, H. P. 2005. Time to abandon dogma: CD14 is expressed by non-myeloid lineage cells. *Immunol. Cell Biol.* 83: 462–467.
4. Weber, C., C. Müller, A. Podszuweit, C. Montino, J. Vollmer, and A. Forsbach. 2012. Toll-like receptor (TLR) 3 immune modulation by unformulated small interfering RNA or DNA and the role of CD14 (in TLR-mediated effects). *Immunology* 136: 64–77.
5. Pugin, J., I. D. Heumann, A. Tomasz, V. V. Kravchenko, Y. Akamatsu, M. Nishijima, M. P. Glauser, P. S. Tobias, and R. J. Ulevitch. 1994. CD14 is a pattern recognition receptor. *Immunity* 1: 509–516.
6. Osterbye, T., D. P. Funda, P. Fundová, J. E. Månsson, H. Tlaskalová-Hogenová, and K. Buschard. 2010. A subset of human pancreatic beta cells express functional CD14 receptors: a signaling pathway for beta cell-related glycolipids, sulfatide and β-galactosylceramide. *Diabetes Metab. Res. Rev.* 26: 656–667.
7. Miller, Y. I., S. H. Choi, P. Wiesner, L. Fang, R. Harkewicz, K. Hartvigsen, A. Boullier, A. Gonen, C. J. Diehl, X. Que, et al. 2011. Oxidation-specific epitopes are danger-associated molecular patterns recognized by pattern recognition receptors of innate immunity. *Circ. Res.* 108: 235–248.
8. Shirey, K. A., W. Lai, A. J. Scott, M. Lipsky, P. Mistry, L. M. Pletneva, C. L. Karp, J. McAlees, T. L. Gioannini, J. Weiss, et al. 2013. The TLR4 an-

tagonist Eritoran protects mice from lethal influenza infection. *Nature* 497: 498–502.
9. Brekke, O. H., and I. Sandlie. 2003. Therapeutic antibodies for human diseases at the dawn of the twenty-first century. *Nat. Rev. Drug Discov.* 2: 52–62.
10. Beck, A., T. Wurch, C. Bailly, and N. Corvaia. 2010. Strategies and challenges for the next generation of therapeutic antibodies. *Nat. Rev. Immunol.* 10: 345–352.
11. Chan, A. C., and P. J. Carter. 2010. Therapeutic antibodies for autoimmunity and inflammation. *Nat. Rev. Immunol.* 10: 301–316.
12. Roopenian, D. C., and S. Akilesh. 2007. FcRn: the neonatal Fc receptor comes of age. *Nat. Rev. Immunol.* 7: 715–725.
13. Nimmerjahn, F., and J. V. Ravetch. 2010. Antibody-mediated modulation of immune responses. *Immunol. Rev.* 236: 265–275.
14. Mueller, J. P., M. A. Giannoni, S. L. Hartman, E. A. Elliott, S. P. Squinto, L. A. Matis, and M. J. Evans. 1997. Humanized porcine VCAM-specific monoclonal antibodies with chimeric IgG2/G4 constant regions block human leukocyte binding to porcine endothelial cells. *Mol. Immunol.* 34: 441–452.
15. Rother, R. P., S. A. Rollins, C. F. Mojcik, R. A. Brodsky, and L. Bell. 2007. Discovery and development of the complement inhibitor eculizumab for the treatment of paroxysmal nocturnal hemoglobinuria. *Nat. Biotechnol.* 25: 1256–1264.
16. Leturcq, D. J., A. M. Moriarty, G. Talbott, R. K. Winn, T. R. Martin, and R. J. Ulevitch. 1996. Antibodies against CD14 protect primates from endotoxin-induced shock. *J. Clin. Invest.* 98: 1533–1538.
17. Thorgersen, E. B., B. C. Hellerud, E. W. Nielsen, A. Barratt-Due, H. Fure, J. K. Lindstad, A. Pharo, E. Fosse, T. I. Tønnessen, H. T. Johansen, et al. 2010. CD14 inhibition efficiently attenuates early inflammatory and hemostatic responses in *Escherichia coli* sepsis in pigs. *FASEB J.* 24: 712–722.
18. Axtelle, T., and J. Pribble. 2003. An overview of clinical studies in healthy subjects and patients with severe sepsis with IC14, a CD14-specific chimeric monoclonal antibody. *J. Endotoxin Res.* 9: 385–389.
19. Reinhart, K., T. Glück, J. Ligtenberg, K. Tschaikowsky, A. Bruining, J. Bakker, S. Opal, L. L. Moldawer, T. Axtelle, T. Turner, et al. 2004. CD14 receptor occupancy in severe sepsis: results of a phase I clinical trial with a recombinant chimeric CD14 monoclonal antibody (IC14). *Crit. Care Med.* 32: 1100–1108.
20. Khodoun, M. V., R. Strait, L. Armstrong, N. Yanase, and F. D. Finkelman. 2011. Identification of markers that distinguish IgE- from IgG-mediated anaphylaxis. *Proc. Natl. Acad. Sci. USA* 108: 12413–12418.
21. Bruhns, P., B. Iannascoli, P. England, D. A. Mancardi, N. Fernandez, S. Jorieux, and M. Daëron. 2009. Specificity and affinity of human Fcgamma receptors and their polymorphic variants for human IgG subclasses. *Blood* 113: 3716–3725.
22. Brekke, O. L., D. Christiansen, H. Fure, M. Fung, and T. E. Mollnes. 2007. The role of complement C3 opsonization, C5a receptor, and CD14 in *E. coli*-induced up-regulation of granulocyte and monocyte CD11b/CD18 (CR3), phagocytosis, and oxidative burst in human whole blood. *J. Leukoc. Biol.* 81: 1404–1413.
23. Brekke, O. L., D. Christiansen, H. Fure, A. Pharo, M. Fung, J. Riesenfeld, and T. E. Mollnes. 2008. Combined inhibition of complement and CD14 abolish *E. coli*-induced cytokine-, chemokine- and growth factor-synthesis in human whole blood. *Mol. Immunol.* 45: 3804–3813.
24. Hellerud, B. C., J. Stenvik, T. Espevik, J. D. Lambris, T. E. Mollnes, and P. Brandtzaeg. 2008. Stages of meningococcal sepsis simulated in vitro, with emphasis on complement and Toll-like receptor activation. *Infect. Immun.* 76: 4183–4189.
25. Thorgersen, E. B., A. Pharo, K. Haverson, A. K. Axelsen, P. Gaustad, G. J. Kotwal, G. Sfyroera, and T. E. Mollnes. 2009. Inhibition of complement and CD14 attenuates the *Escherichia coli*-induced inflammatory response in porcine whole blood. *Infect. Immun.* 77: 725–732.
26. Salvesen, B., J. Stenvik, C. Rossetti, O. D. Saugstad, T. Espevik, and T. E. Mollnes. 2010. Meconium-induced release of cytokines is mediated by the TRL4/MD-2 complex in a CD14-dependent manner. *Mol. Immunol.* 47: 1226–1234.
27. Brekke, O. L., C. Waage, D. Christiansen, H. Fure, H. Qu, J. D. Lambris, B. Osterud, E. W. Nielsen, and T. E. Mollnes. 2013. The effects of selective complement and CD14 inhibition on the *E. coli*-induced tissue factor mRNA upregulation, monocyte tissue factor expression, and tissue factor functional activity in human whole blood. *Adv. Exp. Med. Biol.* 734: 123–136.
28. Meurens, F., A. Summerfield, H. Nauwynck, L. Saif, and V. Gerdts. 2012. The pig: a model for human infectious diseases. *Trends Microbiol.* 20: 50–57.
29. Nunn, M. A., A. Sharma, G. C. Paesen, S. Adamson, O. Lissina, A. C. Willis, and P. A. Nuttall. 2005. Complement inhibitor of C5 activation from the soft tick Ornithodoros moubata. *J. Immunol.* 174: 2084–2091.
30. Barratt-Due, A., E. B. Thorgersen, J. K. Lindstad, A. Pharo, O. Lissina, J. D. Lambris, M. A. Nunn, and T. E. Mollnes. 2011. Ornithodoros moubata complement inhibitor is an equally effective C5 inhibitor in pigs and humans. *J. Immunol.* 187: 4913–4919.
31. Norderhaug, L., T. Olafsen, T. E. Michaelsen, and I. Sandlie. 1997. Versatile vectors for transient and stable expression of recombinant antibody molecules in mammalian cells. *J. Immunol. Methods* 204: 77–87.
32. Sanz, G., E. Pérez, A. Jiménez-Marín, F. Mompart, L. Morera, M. Barbancho, D. Llanes, and J. J. Garrido. 2007. Molecular cloning, chromosomal location, and expression analysis of porcine CD14. *Dev. Comp. Immunol.* 31: 738–747.
33. Summerfield, A., and K. C. McCullough. 1997. Porcine bone marrow myeloid cells: phenotype and adhesion molecule expression. *J. Leukoc. Biol.* 62: 176–185.
34. Berntzen, G., E. Lunde, M. Flobakk, J. T. Andersen, V. Lauvrak, and I. Sandlie. 2005. Prolonged and increased expression of soluble Fc receptors, IgG and a TCR-Ig fusion protein by transiently transfected adherent 293E cells. *J. Immunol. Methods* 298: 93–104.
35. Andersen, J. T., S. Foss, V. E. Kenanova, T. Olafsen, I. S. Leikfoss, D. C. Roopenian, A. M. Wu, and I. Sandlie. 2012. Anti-carcinoembryonic antigen single-chain variable fragment antibody variants bind mouse and human neonatal Fc receptor with different affinities that reveal distinct cross-species differences in serum half-life. *J. Biol. Chem.* 287: 22927–22937.
36. Mollnes, T. E., O. L. Brekke, M. Fung, H. Fure, D. Christiansen, G. Bergseth, V. Videm, K. T. Lappegård, J. Köhl, and J. D. Lambris. 2002. Essential role of the C5a receptor in *E. coli*-induced oxidative burst and phagocytosis revealed by a novel lepirudin-based human whole blood model of inflammation. *Blood* 100: 1869–1877.
37. Barratt-Due, A., E. B. Thorgersen, K. Egge, S. E. Pischke, A. Sokolov, B. C. Hellerud, J. K. Lindstad, A. Pharo, A. K. Bongoni, R. Rieben, et al. 2013. Combined inhibition of complement (C5) and CD14 markedly attenuates inflammation, thrombogenicity and hemodynamic changes in porcine sepsis. *J. Immunol.* 191: 819–827.
38. Lappegård, K. T., D. Christiansen, A. Pharo, E. B. Thorgersen, B. C. Hellerud, J. Lindstad, E. W. Nielsen, G. Bergseth, D. Fadnes, T. G. Abrahamsen, et al. 2009. Human genetic deficiencies reveal the roles of complement in the inflammatory network: lessons from nature. *Proc. Natl. Acad. Sci. USA* 106: 15861–15866.
39. Barratt-Due, A., E. B. Thorgersen, J. K. Lindstad, A. Pharo, O. L. Brekke, D. Christiansen, J. D. Lambris, and T. E. Mollnes. 2010. Selective inhibition of TNF-alpha or IL-1 beta does not affect *E. coli*-induced inflammation in human whole blood. *Mol. Immunol.* 47: 1774–1782.
40. Hamilton, R. G. 1987. Human IgG subclass measurements in the clinical laboratory. *Clin. Chem.* 33: 1707–1725.
41. Schroeder, H. W., Jr., and L. Cavacini. 2010. Structure and function of immunoglobulins. *J. Allergy Clin. Immunol.* 125(2, Suppl 2)S41–S52.
42. Sondermann, P., J. Kaiser, and U. Jacob. 2001. Molecular basis for immune complex recognition: a comparison of Fc-receptor structures. *J. Mol. Biol.* 309: 737–749.
43. Ramsland, P. A., W. Farrugia, T. M. Bradford, C. T. Sardjono, S. Esparon, H. M. Trist, M. S. Powell, P. S. Tan, A. C. Cendron, B. D. Wines, et al. 2011. Structural basis for Fc gammaRIIa recognition of human IgG and formation of inflammatory signaling complexes. *J. Immunol.* 187: 3208–3217.
44. Halloran, P. J., S. E. Sweeney, C. M. Strohmeier, and Y. B. Kim. 1994. Molecular cloning and identification of the porcine cytolytic trigger molecule G7 as a Fc gamma RIII alpha (CD16) homologue. *J. Immunol.* 153: 2631–2641.
45. Qiao, S., G. Zhang, C. Xia, H. Zhang, Y. Zhang, J. Xi, H. Song, and X. Li. 2006. Cloning and characterization of porcine Fc gamma receptor II (FcgammaRII). *Vet. Immunol. Immunopathol.* 114: 178–184.
46. Zhang, G., S. Qiao, Q. Li, X. Wang, Y. Duan, L. Wang, Z. Xiao, and C. Xia. 2006. Molecular cloning and expression of the porcine high-affinity immunoglobulin G Fc receptor (FcgammaRI). *Immunogenetics* 58: 845–849.
47. Stirling, C. M., B. Charleston, H. Takamatsu, S. Claypool, W. Lencer, R. S. Blumberg, and T. E. Wileman. 2005. Characterization of the porcine neonatal Fc receptor—potential use for trans-epithelial protein delivery. *Immunology* 114: 542–553.
48. Vaughn, D. E., and P. J. Bjorkman. 1998. Structural basis of pH-dependent antibody binding by the neonatal Fc receptor. *Structure* 6: 63–73.
49. Kim, J. I., C. J. Lee, M. S. Jin, C. H. Lee, S. G. Paik, H. Lee, and J. O. Lee. 2005. Crystal structure of CD14 and its implications for lipopolysaccharide signaling. *J. Biol. Chem.* 280: 11347–11351.
50. Albright, S., B. Chen, K. Holbrook, and N. U. Jain. 2008. Solution NMR studies provide structural basis for endotoxin pattern recognition by the innate immune receptor CD14. *Biochem. Biophys. Res. Commun.* 368: 231–237.
51. Kelley, S. L., T. Lukk, S. K. Nair, and R. I. Tapping. 2013. The crystal structure of human soluble CD14 reveals a bent solenoid with a hydrophobic amino-terminal pocket. *J. Immunol.* 190: 1304–1311.
52. Köhl, J. 2006. Self, non-self, and danger: a complementary view. *Adv. Exp. Med. Biol.* 586: 71–94.
53. Ricklin, D., G. Hajishengallis, K. Yang, and J. D. Lambris. 2010. Complement: a key system for immune surveillance and homeostasis. *Nat. Immunol.* 11: 785–797.
54. Hawlisch, H., and J. Köhl. 2006. Complement and Toll-like receptors: key regulators of adaptive immune responses. *Mol. Immunol.* 43: 13–21.
55. Hajishengallis, G., and J. D. Lambris. 2010. Crosstalk pathways between Toll-like receptors and the complement system. *Trends Immunol.* 31: 154–163.
56. Song, W. C. 2012. Crosstalk between complement and toll-like receptors. *Toxicol. Pathol.* 40: 174–182.
57. Mollnes, T. E., D. Christiansen, O. L. Brekke, and T. Espevik. 2008. Hypothesis: combined inhibition of complement and CD14 as treatment regimen to attenuate the inflammatory response. *Adv. Exp. Med. Biol.* 632: 253–263.
58. Barratt-Due, A., S. E. Pischke, O. L. Brekke, E. B. Thorgersen, E. W. Nielsen, T. Espevik, M. Huber-Lang, and T. E. Mollnes. 2012. Bride and groom in systemic inflammation—the bells ring for complement and Toll in cooperation. *Immunobiology* 217: 1047–1056.